Cellulose (2010) 17:693–709
DOI 10.1007/s10570-010-9425-7

The glass transition and crystallization of ball milled cellulose

Sabrina S. Paes · Shaomin Sun · William MacNaughtan · Roger Ibbett · Johannes Ganster · Timothy J. Foster · John R. Mitchell

Received: 30 October 2009 / Accepted: 12 May 2010 / Published online: 27 May 2010

Abstract Samples of ball milled cellulose were prepared by ball milling pulps from eucalyptus and softwood (spruce/pine). Water sorption isotherms were obtained by both dynamic vapor sorption and equilibration over saturated salt solutions, in the water content range of 5–42% db (db = dry basis; water as a % age of total solids). Dynamic mechanical analysis using a pocket technique showed a water content dependent thermal transition occurring at the same temperature for the two pulp samples, which was interpreted as a glass transition. Fitting the data to a Couchman–Karasz relationship predicted a value for T_g of the dry cellulose of approximately 478 K, which was similar to values previously reported for other dry polysaccharides. No clear glass transition could be observed calorimetrically, although an endotherm at approximately 333 K was measured, which in polymers is normally attributed to enthalpic relaxation, however the lack of dependence of this endotherm on water content suggests that the melting of some weak associations, such as residual hydrogen bonds, could be a more credible explanation. An exotherm was also observed on heating, which was dependent on water content and which was attributed to partial crystallization of the cellulose. This was confirmed by Wide angle X-ray diffraction and cross polarization magic angle spinning ^{13}C NMR (CPMAS NMR). The recrystallisation was predominantly to form I of cellulose. This was thought to be caused by a small amount of residual form I (probably less than 5%) acting as a template for the crystallizing material. Differential scanning calorimetry reheat curves showed the appearance of freezable water for water contents higher than 20%, as a result of a transfer of water to the amorphous phase following crystallization. The increase in cellulose rigidity following crystallization was also confirmed by CPMAS NMR relaxation. Low resolution proton NMR T_2 relaxation suggested the presence of proton water/cellulose exchange, which was active at water contents of 20% and above.

All the authors are Members of the European Polysaccharide Network of Excellence (EPNOE).

S. S. Paes · S. Sun · W. MacNaughtan · R. Ibbett · T. J. Foster · J. R. Mitchell
Division of Food Sciences, School of Biosciences, University of Nottingham, Sutton Bonington Campus, Loughborough LE12 5RD, UK

Present Address:
S. S. Paes (✉)
Unilever R & D Vlaardingen, Vlaardingen, The Netherlands
e-mail: Sabrina.Paes@unilever.com

S. Sun
Department of Polymer Science and Engineering, Zhejiang University, 310027 Hangzhou, China

J. Ganster
Fraunhofer Institute for Applied Polymer Research IAP, Geiselbergstr. 69, 14476 Potsdam-Golm, Germany

Keywords Amorphous cellulose · Thermal transitions · Ball milling · Crystallinity · Material pockets · DMA

Introduction

Cellulose is one of the most abundant biopolymers in the world and its potential use as a replacement for synthetic polymers has driven recent research regarding cellulosic materials. Cellulose is an unbranched polysaccharide composed of β-1-4 linked glucose units (Purves 1954). Numerous inter- and intramolecular hydrogen bonds form in cellulose because of the large number of polar hydrogen and oxygen atoms (Dumitriu 2005).

Amorphous cellulose has been reported to be produced by ball milling, which is a commonly used mechanical treatment to decrease crystallinity of cellulose and other materials (Ago et al. 2004; Maier et al. 2005; Ouajai and Shanks 2006). Cellulose samples with initially different crystal structures (cellulose I and II) have been found to yield virtually the same amorphous X-ray scattering curves after extensive ball milling (Maier et al. 2005).

The glass transition temperature (T_g) is the temperature below which the physical properties of amorphous materials are similar to those of a solid (glassy state), and above which amorphous materials have liquid characteristics (rubbery state). T_g is one of the most important parameters in understanding mechanical properties of polymers, however, there has been limited research on the T_g of cellulose and amorphous cellulose (Batzer and Kreibich 1981; Goring 1963; Kargin et al. 1960; Ogiwara et al. 1970; Salmen and Back 1977; Szczesniak et al. 2008). Direct experimental measurements of the glass transition temperature of dry amorphous cellulose are not available in the literature, mainly because the temperature range for the main relaxation is close to the degradation temperature of cellulose (Mazeau and Heux 2003). Absorption of water is known to decrease the glass transition temperature of cellulose, as in other biopolymers (Batzer and Kreibich 1981; Salmen and Back 1977; Szczesniak et al. 2008).

Kargin et al. (1960) obtained a glass transition temperature for dry cellulose of about 493 K by extrapolating the solvent dependence of T_g to zero concentration. Goring et al. (1963) determined the T_g of wood cellulose by measuring the changes in the height of a cellulose powder column. With this technique, the T_g values of celluloses from different sources and subject to different treatments were found to be between 504 and 526 K for dry samples. Samples equilibrated over saturated NaCl solutions ($\sim$75% relative humidity) had T_g values between 495 and 512 K (Ibbett et al. 2008). Mazeau and Heux estimated the T_g of dry cellulose to be around 650 K by using molecular modeling (Mazeau and Heux 2003). More recently, Szczesniak et al. (2008) studied the glass transition of microcrystalline cellulose powder at different water contents by DSC. T_g was $\sim$239 K for a sample with a moisture content (wet basis) of $\sim$15% and a 66% crystalline index, which was reported to be in good agreement with the predicted values from Salmen and Back (1977).

Several authors have studied other mechanical relaxations that occur in cellulose, such as the β- and γ-relaxations. The activation energy of the β-relaxation involves dominant entropy contributions while the γ mechanical process is mainly enthalpic in nature (Montes et al. 1997). It was previously reported that the β-relaxation, appeared at temperatures of around 213–253 K (Furuta et al. 2001; Kimura and Nakano 1976; Kubat and Pattyran 1967; Montes et al. 1997; Stratton 1973) and increasing water content shifted the β-relaxation loss peak to lower temperatures, which is similar to the effect on T_g (Montes et al. 1997; Stratton 1973). The decrease in peak size of the β-relaxation with decreasing amount of water implies that the water molecules are acting as more than mere plasticizers (Stratton 1973). Kimura and Nakano (1976) attributed the damping peak between 223 and 253 K to the motion of CH_2OH–H_2O, while the damping peak caused by the motion of CH_2OH was observed at 153 K (γ-relaxation).

Recrystallization of amorphous cellulose is also of great interest (Ago et al. 2004; Hermans and Weidinger 1946; Howsmon and Marchessault 1959; Kimura et al. 1974; Kocherbitov et al. 2008; Ouajai and Shanks 2006; Wadehra and Manley 1965) and can occur by either water absorption (Kimura et al. 1974; Kocherbitov et al. 2008) or heat treatment (Hatakeyama and Hatakeyama 1981; Kocherbitov et al. 2008). Cellulose crystallization has been directly related to the formation of intermolecular hydrogen bonds (Matsuda et al. 1992). It was reported that amorphous cellulose recrystallization to cellulose II occurred after

contact with water or at high relative humidities (RHs) (Kimura et al. 1974; Kocherbitov et al. 2008). Hatakeyama and Hatakeyama suggested that hydration bond formation occurs simultaneously with the rearrangement of cellulose molecules by heat-treatment (Hatakeyama and Hatakeyama 1981). Heat was also found to significantly increase the crystallinity of wood cellulose (Bhuiyan et al. 2000).

The objective of this work was to investigate, using a multi-technique approach, the thermal transitions, reordering and water behavior in cellulose, in order to provide new insights into properties important for cellulose processing and in materials applications.

Materials and methods

Preparation of cellulose samples

Ball milling was used to reduce the crystallinity of cellulose. The majority of the work was carried out on a sample from eucalyptus pulp. Sheets of eucalyptus pulp were kindly supplied by Innovia Films Ltd (Wigton, UK). Cellulose pulp was firstly cooled with liquid nitrogen and cut into smaller pieces in a kitchen electric mill. This was followed by a second pre-milling at 600 rpm for 30 min in a Planetary Micro Mill (Pulverisette 7, Fritsch, Germany), in order to obtain a crude powder of reduced bulk, and to decrease the volume of the soft material. Ball-milling to very low crystallinity was performed with $\sim$1 g of pre-milled powder in agate bowls (12 mL volume) with agate balls (10 mm diameter), at 600 rpm for 10 h, with cycles of 30 min milling and 30 min pausing. The ball milling was divided into short periods principally to avoid excessive heating. X-Ray patterns were recorded to investigate the level of crystallinity and whether the samples were truly amorphous after the ball milling.

The second sample was obtained from softwood (Modo, Domsjö, Sweden) and prepared by the Fraunhofer Institute (Berlin, Germany). The original softwood pulp was composed of a mixture of Norwegian spruce and Scottish pine (60 and 40%, respectively). These samples were ball milled for 8 h at a frequency of 40 Hz (2,400 rpm). The molecular sizes/degrees of polymerization (DP) were determined by Standard Cuen and Cuoxam methods, the details of which can be found in Drechsler et al. (2000). Molecular sizes of the two cellulose samples are shown on Table 1.

Sample equilibration and sorption isotherms

Sample equilibration

Samples were equilibrated isopiestically over saturated salt solutions to give moisture contents in the range 5–42% db (db = dry basis; water as a percentage of total solids). The water contents were determined by heating the equilibrated samples to dryness in an oven at 378 K. The sorption isotherm was obtained by plotting the water content values at equilibrium and the water activity a_w (=RH/100%) provided by each saturated salt solution.

Dynamic vapor sorption

A dynamic vapor sorption analyzer (DVS) (Surface Measurement Systems Ltd, London, UK) equipped with a Cahn D200 microbalance was used to measure

Table 1 Molecular size, expressed in terms of the degree of polymerization (DP), and water contents of the original and ball milled cellulose pulps

	Water content (% db)	DP-Cuen	DP-Cuoxam
Eucalyptus (original)	6	935/928	539/535
Eucalyptus (ball milled)	6	563/569	332/335
Softwood (original)	6	1,186	678
Softwood (ball milled)	14	218	140

Where 2 values are shown these represent the results of 2 separate determinations

the water sorption isotherms of the cellulose samples. The experiments were carried out at a temperature of 298 K and relative humidities ranging from 0 to 90%. The initial weight of the samples was approximately 20 mg. Samples were pre-dried in the DVS by passing dry air over the powder until equilibration. The dry samples were subsequently hydrated in RH steps of 10%. Samples were considered equilibrated when the change in mass per unit time was less than 0.0005 mg/min or the equilibration time had reached 1,500 min. Using this procedure, the moisture content could be plotted against RH and the isotherm obtained.

The form of the isotherm curves can be described using various equations. In this work the Guggenheim, Anderson and De Boer (GAB) model was used in order to describe different hydration stages in the ball milled cellulose. The GAB model is expressed mathematically in Eq. 1:

$$M = \frac{M_0 C K a_w}{(1 - K a_w)(1 - K a_w + c K a_w)} \quad (1)$$

where M is the equilibrium moisture content (in db), M_0 is the water content in the monolayer, a_w (=RH/100%) is the water activity C is a constant related to the monolayer enthalpy of sorption, and K is a constant related to the multilayer heat of sorption. The constants C and K are temperature dependent (Rizvi 1994; Van den Berg and Bruin 1981; Yakimets et al. 2007).

The GAB model can be split into contributions from multilayer and monolayer water content, according to the following equations (Kent and Meyer 1984):

$$M_0 = M(1 - K a_w) \quad (2)$$

$$M_{mult} = M K a_w \quad (3)$$

where M_0 and M_{mult} are the equilibrium moisture content in the monolayer and multilayer, respectively (db).

The goodness of fit was evaluated using the mean relative deviation modulus (P), defined by:

$$P = \frac{100}{n} \sum \frac{|M_i - M_{Ei}|}{M_i} \quad (4)$$

where M_i is the experimental moisture content of experiment i, M_{Ei} is the predicted moisture content, and n is the number of experiments (Lomauro et al. 1985; Perez-Alonso et al. 2006).

Thermal transitions

Dynamic mechanical analysis

Dynamic mechanical analysis (DMA) was conducted at a frequency of 10 Hz with two different Mechanical Analyzers (a DMA MK II head with MK III electronics, from Rheometric Scientific, UK and a DMA8000, from Perkin Elmer, USA). The values of modulus and Tan γ obtained from both machines were identical within experimental error. A material pocket technique (Raschip et al. 2008; Royall et al. 2005) in single cantilever geometry, at a heating rate of 2 K/min was used. The cellulose powders at different water contents were distributed evenly inside the pockets, the pocket folded shut, and the sample covered with silicon oil to minimize moisture loss during the test.

In the cantilever mode, the sample is subject to shearing between the 2 outer steel layers. This is an invaluable method, if the sample is difficult to prepare in an accurate shape, such as ball milled cellulose; it being very much easier to distribute a fine powder inside a pocket than to form a bar from a dispersed fibrous or powdered sample. Whilst observation of temperature transitions may be accurate, the sample moduli (E') are relative only, reflecting the contribution from the stiff material used in the pocket, superimposed on the much smaller changes of the sample.

Differential scanning calorimetry

Thermal transitions were monitored using a heat flux Mettler Toledo DSC 823e (Leicester, UK) with auto sampler and liquid nitrogen cooling attachment. Samples were transferred rapidly from equilibration boxes to 40 µl aluminium pans to ensure minimal changes in water content, and were typically run from temperatures of 233–423 K at scan rates of 10 °C min^{-1} with reheats being carried out. The machine was calibrated for temperature using the onset temperatures of melting in indium and cyclohexane and for heat flow using the enthalpy of transition of indium. Enthalpy and T_g values were calculated using Mettler Toledo Star^e software.

Micro-differential scanning calorimetry

Micro-differential scanning calorimetry (*Micro*-DSC) was used in this study principally to provide sufficient

amounts of material, crystallized in a controlled fashion, for X-Ray and solid state NMR studies. *Micro*-DSC is distinguished from "conventional" DSC by the increased sensitivity of the machine, larger sample volumes and lower scan rates The experiments were performed in a *Micro* DSC III (Setaram, Caluire, France) using cells made from Hastalloy, capable of holding approximately 0.8 mL. Heat and temperature calibrations were carried out electrically on this machine and could not be changed by the user. However, the values could be checked using the transition in naphthalene.

Powders were packed into the cell and initially cooled to a starting temperature of 273 K. Samples were run at rates of 1 K/min up to 373 K. The reference cell was filled with water and matched for heat capacity with the sample. This ensured that the calorimeter was balanced and that the heat flow signal was centered around the zero level which gives the most sensitive result.

Wide angle X-Ray diffraction

Samples were prepared by filling plastic holders with randomly oriented powders. X-Ray measurements were carried out on a Bruker D5005 diffractometer (Bruker AXS, UK) using copper K alpha (CuKα) radiation of wavelength 1.5418 Å. Slit focus reflection geometry was used.

Crystallinity determination was performed by firstly applying a linear background over the range of the main diffraction features. The diffraction peaks were then simulated as a series of pure Gaussian functions. For cellulose I these represent the $1\bar{1}0$, 110 and 200 crystallographic planes whilst for cellulose II they represent $1\bar{1}0$, 110 and 020 planes. One broad pure Gaussian feature was used for the amorphous component. This method is based on the procedure in reference (Öztürk et al. 2009). Positions and relative intensities were restricted to typical values for Cellulose I and II diffraction peaks, whilst width and group intensity were allowed to vary independently. Slight variations in position were due to small errors in the height of samples. In this way an estimate of the relative contents of Cellulose I and II allomorphs could be obtained for the nominally amorphous as well as recrystallized samples. The data manipulation was carried out using intensity vs. 2θ data in the *Microsoft Excel* software package with the *Solver* add in.

Low resolution proton NMR

Low resolution Proton NMR was carried out on a RI Maran benchtop spectrometer operating at 23 MHz (Oxford Instruments, Tubney Woods, UK). 90° pulse lengths were approximately 3 μs with repeat times of 4 s. For simple free induction decay measurements 4 K of data were normally collected with dwell times of 1 μs. Accurate T_2 values were determined using a Carr Purcell Meiboom Gill (CPMG) pulse sequence with a single τ value of 256 μs and typically 2,048 echoes. Data was fitted to single exponential decay curves using RINMR software. T_1 measurements were made using an inversion recovery pulse sequence with appropriately spaced delay times.

^{13}C cross polarization magic angle spinning nuclear magnetic resonance (CPMAS NMR)

CPMAS mobility measurements

Instead of the usual range of 10–15 values in a variable contact time experiment, 2 discrete contact time values have been chosen in the present experiments. These were 1 ms—a value which is often close to the maximum transfer of polarization, and 5 ms—a value which should produce a substantial drop in intensity due to motional processes. In these cellulosic materials, which are on the solid side of the minima produced by T_1 processes, a lower value of the $T_{1\rho}$ is returned by samples having a greater mobility.

The parameters used in these experiments were as follows. The Proton 90° pulse length was 6–7 μs. Contact time for the variable contact time motional experiment was either 1 or 5 ms. Field strength of the proton and spin locking fields was 42–36 kHz. Samples were packed into 7 mm rotors and spun at speeds of 4 kHz. Reference ppm scales were provided, using the high field line of adamantane (29.5 ppm) run under identical conditions to the samples.

Data processing

1 K of data points were normally recorded. On data processing this data set was zero filled to 4 K and 20 Hz of Lorentzian line broadening applied. The data set was Fourier transformed and phased with 0 and 1st order corrections. Polynomial baseline fitting

was consistently applied to all spectra under the peaks of interest.

The C4 region of the spectra was used for assessing the crystalline and amorphous content of the cellulose and for data fitting, Parameters for simulated Gaussian peaks were adjusted via automated non-linear least-squares minimization using Microsoft Excel Solver. Due to the dry nature of the samples, the spectra were not of sufficient resolution to be used per se to unequivocally determine the number of peaks composing the C4 region. Instead, the assignments of spectral peaks in several references in the literature were used (Earl and VanderHart 2002; Larsson et al. 1997; Newman and Hemmingson 1995). It was found that a simplified assignment of broad peaks covering 3 areas; crystalline, disordered and partially disordered was sufficient to describe most of the C4 environments of materials containing predominantly the cellulose I allomorph. Manual intervention was occasionally required during fitting and was essential for the selection of appropriate starting values.

Results and discussion

Sorption isotherms as a monitor of the state of water

The isotherm for ball milled cellulose (eucalyptus) together with the GAB model fit up to an RH of 90% (Eq. 1), are shown on Fig. 1a and b. A comparison of the isotherms for ball milled cellulose (eucalyptus) obtained by DVS and isopiestic methods is also shown on Fig. 1a.

The agreement between both methods was tolerably good. The equilibrium RH in the isopiestic method can be affected by imperfect sealing of the humidity boxes and contact with ambient RH ($\sim$60%), so it was expected that water contents below ambient RH could be slightly raised Therefore, for the isopiestic method the isotherm may be slightly shifted to the left on the graph compared to the isotherm determined by DVS. The GAB parameters are shown on Table 2. The goodness of fit of the equations to the data was determined using the mean relative deviation modulus (P) (Eq. 4) (see Yakimets et al. 2007 for further details). The fitted parameters to the isotherm give an idea of the availability of water.

Also shown in Fig. 1b is the isotherm for a sample equilibrated at 54% RH and subsequently heated to 373 K. The sample was partially recrystallized as confirmed by X-ray and other techniques (see following discussion). The isotherm for the recrystallized sample was at a lower level than that for the unheated ball milled sample, which is to be expected as the crystallized fraction is anhydrous and should only contribute weakly to the isotherm by a small amount of surface adsorption. The shift of the sorption isotherm to lower values of water contents when recrystallization occurs is also observed in starch (Stute 1992). The isotherms will be discussed

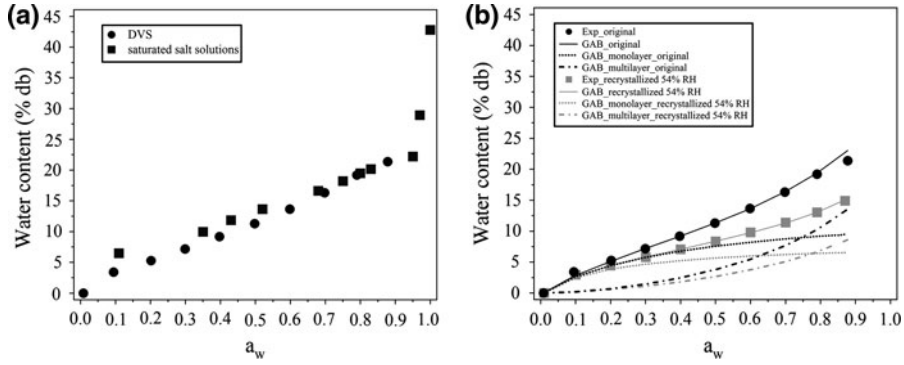

Fig. 1 Sorption isotherms for **a** eucalyptus ball milled cellulose determined using DVS and saturated salt solutions and **b** for the same material equilibrated at 54% RH and subsequently heated in a controlled manner at 1 K/min in a Setaram Micro-DSC from 283 to 373 K. The experimental values are shown as *symbols*; the fits with the GAB model are shown as *solid lines*. The *dotted lines* represent the monolayer contribution and the *dashed lines* the multilayer contribution to the overall water content

Table 2 GAB parameters from the fitted sorption isotherms, compared with literature values

	GAB			
	M_0 (db)	C	K	P
Eucalyptus ball milled cellulose	11	4.39	0.67	1.26
Recrystallized eucalyptus cellulose	7	7.71	0.65	0.38
Literature				
Cellulose (Parchment paper) (Despond et al. 2005)	6	16.8	0.75	–
Microcrystalline cellulose (58% crystallinity) (Agrawal et al. 2004)	4	10.6	0.74	–
Microcrystalline cellulose (Van den Berg 1984)	8	16.6	0.81	–
Microcrystalline cellulose (Van den Berg 1984)	8	24.3	0.81	–

M_0 = monolayer value. See text for definitions of C, K and P. The recrystallized sample was equilibrated at 54% RH and heated at 1 K min^{-1} from 283 to 373 K in the Setaram micro-DSC

with reference to the low resolution proton NMR results in a later section.

The individual contributions of monolayer and multilayer water to the overall isotherm, as described by Eqs. 2 and 3, are also shown on Fig. 1b. The amount of water in the monolayer M_0 for the recrystallized sample was lower than that obtained for the unheated ball milled sample as shown in Table 2. For both samples the amount of water present as a multilayer rapidly increased at around 0.3 a_w, but with a higher absolute water content for the unheated ball milled cellulose. At $a_w \sim 0.90$ a steep increase of water content was observed for the eucalyptus ball milled cellulose. GAB parameters for the recrystallized sample were also closer to the values previously reported for crystalline cellulose (Agrawal et al. 2004; Rahman 1995; Van den Berg 1984), which supports the view that initial partial recrystallization occurred after heat treatment.

Thermal transitions

T_g: Dynamic mechanical analysis

Figure 2 shows apparent values for Tan δ and the storage modulus (E') as a function of temperature. Although the values have only relative meaning, the change in these parameters with temperature can be used to monitor thermal transitions in the powder (Royall et al. 2005; Raschip et al. 2008). The DMA results provided good evidence for an underlying glass transition in the region of 320–380 K, as demonstrated by the water content dependence, and less convincingly of a crystallization event or possibly a second glass transition of a rigid amorphous fraction at higher temperatures. The second transition at around 390 K appeared to be only weakly water dependent. Although every effort was made to prevent water loss, it is possible that at this high temperature, compounded by the slow scan rate, all

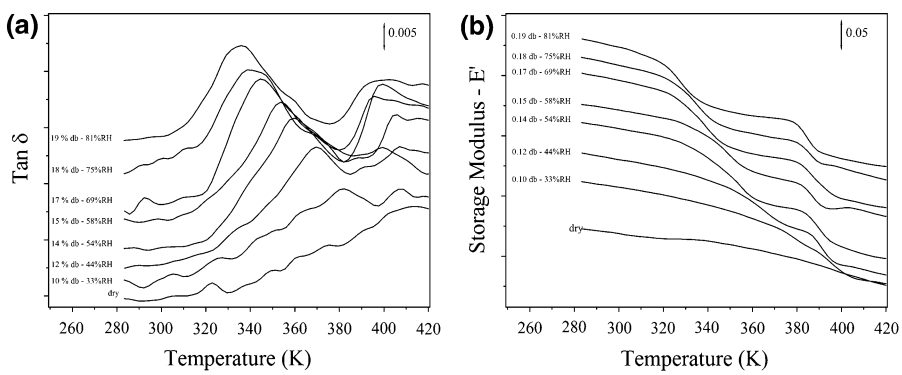

Fig. 2 **a** The tan delta peak and **b** the Young's storage modulus E' as a function of temperature. Both the water content expressed as a dry basis and the corresponding RH are shown. Note the two transitions observed for all but the lowest moisture content and how the lower temperature transition is more temperature sensitive

samples had similar water contents due to drying. This mechanical transition could therefore be due to recrystallisation of constant moisture content samples. The possibility also exists that this event is a second glass transition although this would normally be expected to be water content dependent. However, if this were a glass transition of a rigid fraction, then perhaps the water content dependence would be less and could be described by changes in the values of the parameters in the Couchman–Karasz equation. This remains to be investigated but will be discussed further in the light of the DSC and CPMAS NMR results.

Figure 3 displays the lower temperature transition temperature, defined by the peak in Tan δ, as a function of water content. As would be expected from a consideration of mechanical properties, the drop in the storage modulus (E') is observed at somewhat lower temperatures. Good agreement is obtained between the two cellulose samples despite the widely different molecular weights. This was expected, as the glass transition temperature should be independent of polymer size in this range (DP > 200), as has been found in starch like polymers (Lazaridou et al. 2003; Orford et al. 1989).

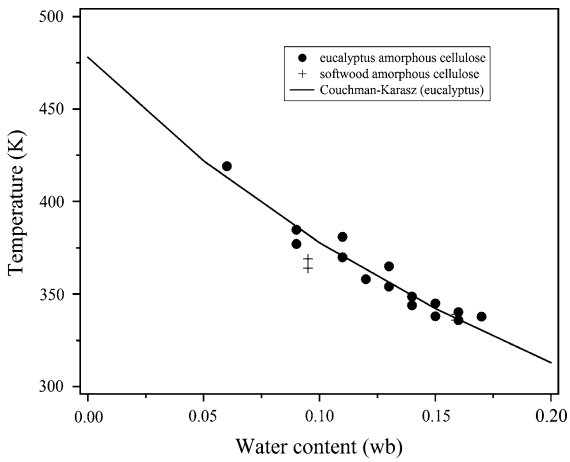

Fig. 3 The glass transition temperature as a function of water content expressed on a wet basis. The water content is expressed on a wet basis for the Couchman–Karasz model as the equations are in terms of overall fractions of water and polymer. T_g was determined as the peak in tan delta of the lower temperature transition from the dynamic mechanical analysis results in Fig. 2. Data is shown for both eucalyptus and softwood ball milled cellulose samples. The *solid line* is the fit from the linear version of the Couchman–Karasz equation (see text for details)

The data in Fig. 3 were fitted by the automated non linear least-squares method in Excel Solver. The Couchman–Karasz equation (Eq. 5) was used to estimate the value of T_g for dry amorphous cellulose. The Couchman–Karasz equation is expressed as (Couchman and Karasz 1978):

$$T_g = \frac{w_1 \Delta C_{p_1} T_{g_1} + w_2 \Delta C_{p_2} T_{g_2}}{w_1 \Delta C_{p_1} + w_2 \Delta C_{p_2}} \quad (5)$$

where w_1 is the weight fraction of water (diluent), w_2 is the weight fraction of the amorphous cellulose (polymer), T_{g_1} is the glass transition of water, T_{g_2} is the glass transition of the amorphous cellulose (dry), ΔC_{p_1} is the change in heat capacity of water at T_{g_1} (equal to 1.94 J/g K) and ΔC_{p_2} is the change in heat capacity of the amorphous cellulose at T_{g_2}.

By restricting the fitting range for values of T_g and ΔC_p to those thought reasonable for other polysaccharides, we obtained values of 478 ± 12 K and 0.54 ± 0.05 J/g K, respectively. This was a typical value for the T_g for dry polysaccharide polymers, but a slightly high value for ΔC_p, 0.2–0.3 J/g K being more usual. These values are similar to those suggested by Orford et al. (1989) for amylose and amylopectin namely a T_g of 500 ± 10 K and a ΔC_p of 0.47 J/g K.

Table 3 shows the values for the T_g and ΔC_p for dry polysaccharides such as starch and cellulose. Values from the literature were converted to the same units to aid comparison. These were calculated using different methods such as molecular modeling and fitting by similar models to the Couchman–Karasz equation.

Calorimetric and mechanical transitions in ball milled cellulose as determined by DSC and DMA

We were not able to detect a glass transition calorimetrically, which was in agreement with several previous studies (Gidley et al. 1993; Roos 1995; Stubberud et al. 1996), although not with the recent report by Szczesniak et al. (2008). The first heat thermograms for both ball milled cellulose samples, softwood and eucalyptus, are shown in Fig. 4a and b.

Although rheological methods can be up to a thousand fold more sensitive than calorimetric

Table 3 Literature values for T_g and ΔC_p for dry polysaccharides showing the respective methods used and the references

	T_g dry state (K)	ΔC_p (J/g K)	Method	Reference
Ball milled cellulose	478	0.54	Couchman–Karasz	This work
Pea amylose	605	0.265	Couchman–Karasz	Bizot et al. (1997)
Potato starch	589	0.265	Couchman–Karasz	Bizot et al. (1997)
Waxy maize starch	558	0.161	Couchman–Karasz	Bizot et al. (1997)
Amylose	500 ± 10	0.47	Ueberreiter and Kanig	Orford et al. (1989)
Amylopectin	500 ± 10	0.47	Ueberreiter and Kanig	Orford et al. (1989)
Cellulose			Experimental	Goring (1963)
Avicel	526			
Bleached spruce sulphite pulp	504			
Unbleached spruce kraft pulp	518			
Cellophane	517			
Hollow filament rayon	510			
Cellulose	526			
Amorphous cellulose	500	–	Molecular modeling	Chen et al. (2004)
Cellulose	493		Experimental	Kargin et al. (1960)

Some values have been converted to more usual units to aid comparison

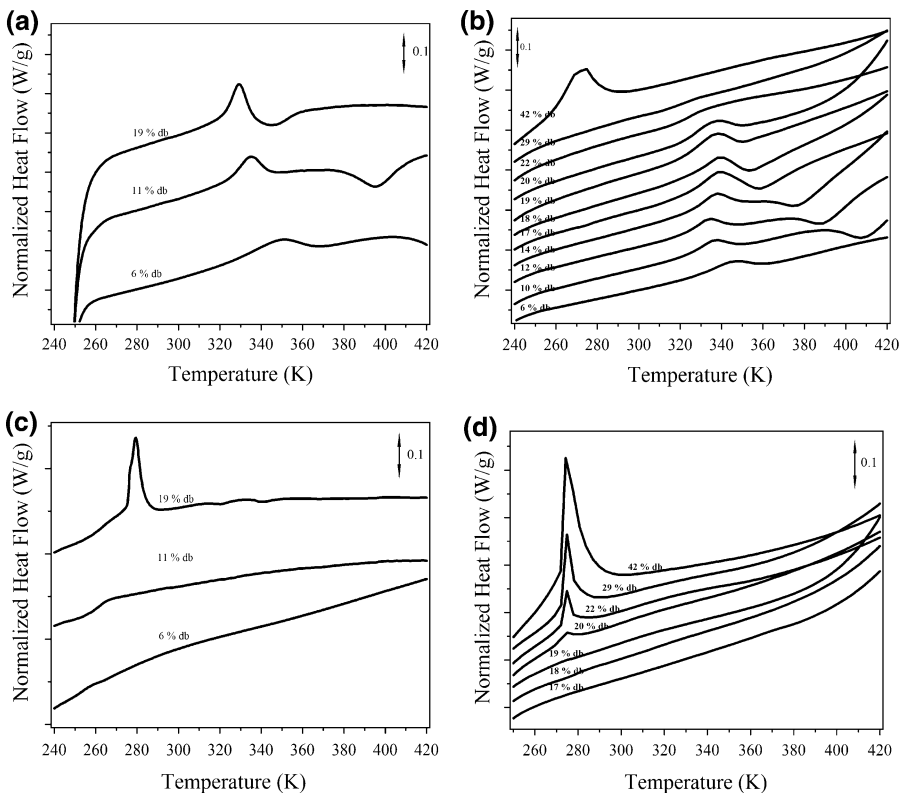

Fig. 4 First heating runs for ball milled **a** softwood and **b** eucalyptus celluloses. The second heating runs for **c** softwood and **d** eucalyptus celluloses are also shown. The samples were equilibrated over salt solutions. See Table 5 for corresponding moisture/RH values. Endothermic heat changes are *plotted upwards*. Notice the low temperature endotherms, the onset temperatures of which are close to 273 K

methods, this may not be the only reason why these transitions are comparatively easy to observe rheologically but difficult to observe calorimetrically. Tan δ (Fig. 2) showed very broad transitions—from 303 K to over 373 K in the case of the sample with water content 19% db. The scanning rate for these

measurements was necessarily low (2 K/min), which will also compound any spread transitions due to sample drying during measurement. However, if the breadth of the transition is a true reflection of the properties of the sample, then in the DSC measurement the naturally low values of ΔC_p at the transition will be spread over a wider temperature range with the concomitant problems of baseline slope and curvature further increasing the difficulty of the calorimetric observation.

At higher temperatures, it is possible that progressive drying in all the samples exacerbated by the slow scan rate, moved all crystallization events to higher temperatures as the sample dried. The sample is only poorly sealed by an oil barrier in the DMA method but hermetically sealed in the DSC pan. This may be the cause of the second transition which appears at roughly a constant temperature for all samples (Fig. 2b), namely the crystallization of dried samples, all at a similar moisture content. Naturally the drying is not so critical at lower temperatures where the glass transition is observed.

The interesting possibility also exists that this second higher temperature transition is the glass transition of a restricted mobility amorphous fraction. We found evidence for a restricted mobility fraction in the CPMAS traces (see Figs. 6, 7 and the supporting discussion) corresponding to previously assigned accessible and inaccessible disordered surfaces or ends of crystallites.

Figures 4a and b show the first heating run DSC curves for both ball milled cellulose samples. The endotherm at approximately 333 K is frequently observed in thermograms of polysaccharides and, among other interpretations, has been postulated to be due to a physical ageing or enthalpic relaxation peak (Appelqvist et al. 1993; Bizot et al. 1997; Shogren 1992). There is a tendency to ascribe peaks such as these in amorphous polymers and biopolymers to physical ageing, however the lack of water content dependence particularly in the eucalyptus sample is puzzling.

Physical ageing in polysaccharides has seen extensive work and modeling, using models from the polymer literature such as the Tool Narayanaswamy Moynihan (TNM) approach (Noel et al. 2005). This has shown that depending on the values of the particular parameters chosen, in particular the x or non-linear parameter, the ageing peak can appear above or even just below the temperature region of T_g. Essentially this approach is looking at time dependence in the transition region. However, it would be surprising in an experiment involving a systematic change of moisture content, for TNM model parameters to change in such a way as to leave the ageing peak in the same position whilst the underlying T_g changed. This is possible but surprising. As the glass transition changes in temperature as a function of moisture content, so the ageing peak would be expected to follow. This therefore argues against the conventional interpretation of the peak as an ageing peak. It may be that there are some weak associations still present, probably involving hydrogen bonds which can be "melted" out and so contribute to a constant temperature endotherm. The temperature of ageing peaks is an unreliable indicator of the temperature of an underlying and invisible T_g.

The recrystallization of ball milled cellulose

Ball milled cellulose samples equilibrated at 54 and 80% RH were recrystallized in the *Micro*-DSC by heating in a controlled manner. The cells in the Micro-DSC are able to hold approximately 0.8–0.9 mL. Sufficient sample was therefore available to use directly for the X-Ray and CPMAS measurements presented in Figs. 5, 6, and 7. Furthermore, a direct recorded history of the sample including the temperature profile and data

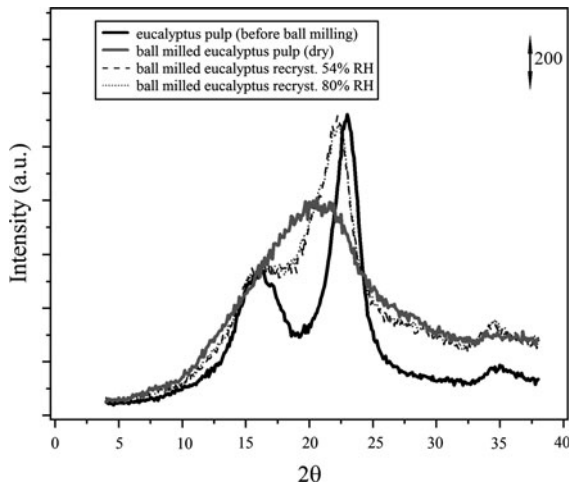

Fig. 5 X-ray diffractograms of the original eucalyptus cellulose before and after ball milling and samples equilibrated at 54 and 80% RH which have been recrystallized in the Micro-DSC

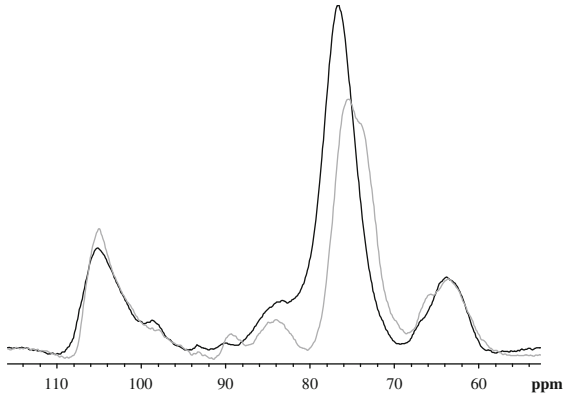

Fig. 6 Base line corrected CPMAS traces showing ball milled (*dark curve*) and 54% RH recrystallized ball milled eucalyptus cellulose (*light curve*). Both of these spectra were recorded at a contact time of 1 ms. The C4 region, which was used for the fitting of Gaussian curves to describe the crystalline and amorphous components, lies in the 80–92 ppm region

on the extent of crystallization was available (data not shown). Figure 5 shows X-Ray diffractograms of the original eucalyptus cellulose before and after ball milling and samples recrystallized in the *Micro*-DSC. Figures 6 and 7 show CPMAS NMR data for a sample equilibrated at 54% RH before and after recrystallization in the *Micro*-DSC.

The X-Ray patterns hinted at the presence of both forms I and II of cellulose in the recrystallized traces. The evidence for this included changes in relative peak intensities and the slight shift of the higher angle peak from a 2θ value of approximately 23.0° (close to cellulose I 200) to a lower value of $2\theta \sim 22.0°$ (close to cellulose II 020). In addition a slight shoulder was present in the region of $2\theta \sim 12°$, indicative of the presence of a small amount of form II.

In some ways this is a surprising result. Cellulose is generally thought to recrystallise in the type II form. That the predominant recrystallisation here is into type I probably implies that the residual amount of type I in the nominally amorphous cellulose (see Table 4) is acting as a template on which the amorphous material can crystallize. The nominally amorphous material showed evidence of small amounts of crystalline material, once again through the presence of shoulders on the trace. This could be fitted by assuming standard diffraction patterns for forms I and II and optimizing these together with an amorphous background to the diffraction pattern of the ball milled material.

We have also measured the effective molecular size of the material before and after ball milling. Although there is still some crystalline material present in the nominally amorphous material, it is not desirable to ball mill indefinitely to remove the last remaining fraction, as the molecular size has already decreased under the present conditions. Fortunately parameters

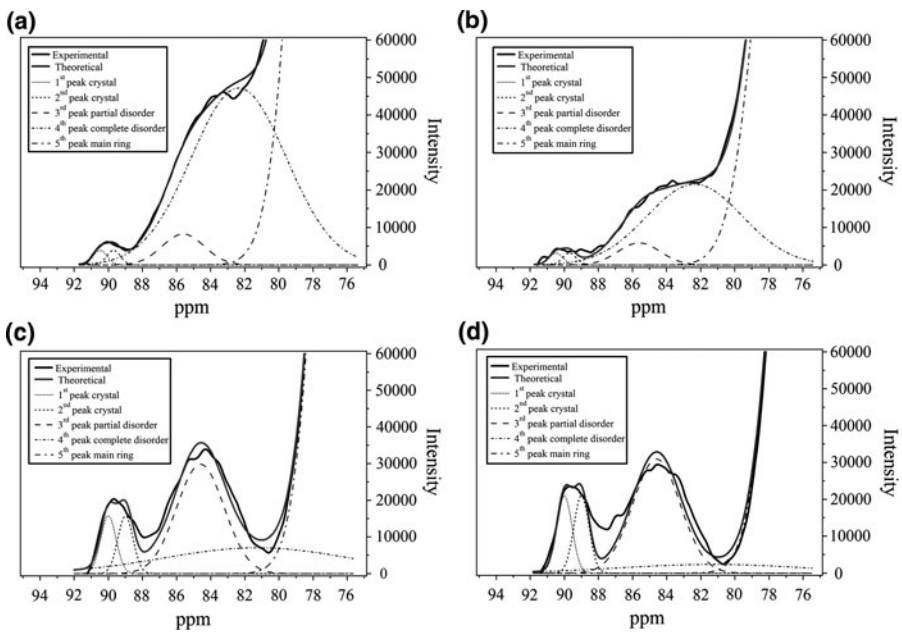

Fig. 7 **a–d** CPMAS spectra at various contact times showing, respectively. **a** Ball milled Eucalyptus cellulose, equilibrated at 54% RH, before crystallization. Contact time 1 m. **b** Ball milled Eucalyptus cellulose, equilibrated at 54% RH, before crystallization. Contact time 5 m. **c** Ball milled Eucalyptus cellulose, equilibrated at 54% RH, after crystallization. Contact time 1 m. **d** Ball milled Eucalyptus cellulose, equilibrated at 54% RH, after crystallization. Contact time 5 m

Table 4 Positions of the CPMAS NMR peaks for the fitting procedures corresponding to Fig. 7, and the various crystalline ratios for the ball milled eucalyptus samples at 54% RH

CPMAS NMR Sample/contact time	Peak 1 Xall C	Peak 2 Partial P	Peak 3 Disordered D	Crystallinity C/P (%)	Crystallinity C/(P + D) (%)
Ball milled 1 m	90	85.6	82.3	31	2.2
Ball milled 5 ms	90	85.6	82.3	–	–
Xall 1 ms	89.5	84.6	81.3	33.8	19.2
Xall 5 ms	89.5	84.6	81.3	–	–

X-ray	Type I polymorph % Total	Type II polymorph % Total	Crystallinity C/(C + A) % total
Eucalyptus (original)	48	–	48
Eucalyptus nominally amorphous (ball milled)	<2	<4	<6
Recrystallized eucalyptus ball milled cellulose 54%	24	7	30
Recrystallized eucalyptus ball milled cellulose 80%	22	8	30

Crystallinity values for 1 ms contact time only are given. Also shown are comparable X-ray measurements on crystallinity for a series of cellulose samples. The recrystallised samples were heated at 1 K/min in a Setaram Micro-DSC from 283 to 373 K

C Crystalline, *P* partially disordered, *D* disordered, *A* amorphous

such as the glass transition are not particularly sensitive to molecular size. We have given careful consideration to the issue of ball milling and the remaining level of crystalline material. A superficially broad featureless amorphous looking peak may conceal a small amount of crystalline material sufficient to act as a template for crystallization. Similarly a truly amorphous peak lacking any features may represent a substantially degraded sample.

Crystallization was only partial and complete recrystallization was not observed at any water content or heating regime. Approximate values for X-Ray and CPMAS NMR determined crystallinity values are given on Table 4.

The dynamics of the CPMAS experiment must be considered before absolute measurement of peak intensities or areas. Clearly at 5 ms contact time (Fig. 7b, d), the peaks representing the mobile (usually amorphous) regions will have decayed, returning an erroneous value for the crystallinity. Therefore, a value of 1 ms contact time (Fig. 7a, c) was chosen, as being near the optimum for

Table 5 Enthalpy values calculated from the DSC traces (Fig. 4)

Water content/ RH % db/% RH	Enthalpy of ~333 K endotherm (J/g)	Enthalpy of exotherm (J/g)	Enthalpy of endotherm on reheat (J/g)	Crystallinity by X-ray diffraction (%)	Water content of Amorphous phase (% db)
6/11	1.56		–	–	–
10/33	1.37	3.22	–	–	–
12/43	1.69	5.32	–	–	–
14/54	2.11	7.77	–	30	20
17/69	1.88	2.09	–	–	–
18/75	1.34	1.64	–	–	–
19/80	1.15	0.52	0.58	30	27
20/83	0.93	0.22	0.53	–	–
22/95	–	–	2.16	–	–
29/97	–	–	4.26	–	–
42/100	–	–	10.62	–	–

The water content calculation in the amorphous phase was based on the complete exclusion of water from the Crystalline material

quantitative calculation, however dynamic effects are still present in any CPMAS experiment and will introduce significant errors.

As a further method of comparison of crystallinity, Table 5 shows the enthalpy values for the crystallization exotherm and X-Ray estimates of the level of crystallization for both recrystallized samples. At higher moisture contents (>16% db) the exotherm appeared to be occurring beneath the endotherm at 333 K, making it impossible to accurately calculate the energy of the exothermic transition. This can be seen in the case of recrystallization at 80% RH, where despite the crystallization value being 30%, the exotherm enthalpy is only ~0.5 J/g.

Figure 4d shows DSC scans for reheating the partially crystallized material (eucalyptus). As would be expected, any slow physical ageing response is absent. However, from the endotherm at 273 K, clear evidence for the presence of meltable/freezable water is present for samples with a water content >19% db. An equivalent melting peak is only seen for the first heating runs of ball milled samples at higher water contents; between 29 and 42% db from Fig. 4b. In a closed system, the development of a dehydrated crystalline cellulose fraction will release water into the remaining amorphous phase, raising the amorphous region water concentration. If the water level is sufficiently high that any non-freezing water component reaches saturation, any additional water transferred into this region will have normal melting behavior. The total amount of water in the amorphous phase following recrystallization can be calculated from the XRD value for crystallinity, and the total initial water content, as shown in Table 5 for the samples equilibrated at 54 and 80% RH. From this it appears that meltable/freezable water is observed when the water content of amorphous cellulose exceeds about 30% db, or around the expected non-freezing water capacity of 3 water molecules for 1 anhydroglucose unit.

The higher temperature DSC thermal transitions involving cellulose (Fig. 4c, d) could not be observed on partially crystallized material, i.e., on a reheat of the crystallized material. They were also not observed by DMA. In combination with the CPMAS NMR results (Fig. 7), this suggested that either the cellulose has thermally degraded or the amorphous component in the recrystallized cellulose has now substantially less mobility than in the original ball milled material rendering the change in heat capacity still smaller and the transition temperature yet higher and possibly spread over a wider temperature range.

Having now considered the thermal transitions in ball milled cellulose including the glass transition and recrystallization, it is instructive to plot these 2 parameters together. Figure 8 shows that the temperature of the onset of recrystallization, as determined by DSC, is always above (by about 15–20 °C) that of the glass transition determined by DMA. This is broadly consistent with studies on synthetic polymers which state that cold crystallization occurs when there is sufficient mobility in the system such that the molecules can overcome an energy barrier and attain a lower energy configuration in a crystal. The temperature at which this occurs is between the glass transition temperature and the Melting temperature. However, Fig. 8 is complex as the respective frequencies of measurement of T_g and recrystallisation (dependent on an underlying T_g) are not comparable. The DSC is run at 10 °C min^{-1} whereas the DMA measurements are made at a frequency of 10 Hz. Whilst there is no exact way of comparing these values, the DSC probably corresponds to a lower frequency measurement. Therefore, while it may appear that the recrystallisation is a surprisingly rapid process and occurring at a slightly higher temperature that T_g in actual fact the temperature separation of these two events should probably be greater.

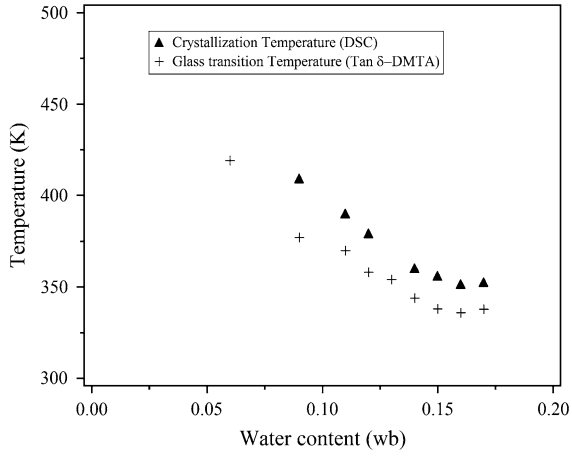

Fig. 8 The glass transition midpoint temperature as determined by DMA (peak in tan δ at 10 Hz) plotted with the corresponding onset of crystallization temperature as determined by DSC (10 °C min^{-1})

^{13}C CPMAS NMR, order and mobility

The analysis of the CPMAS data was carried out using a similar approach to Ibbett et al. (2007), as applied to regenerated cellulose, where three separate morphological assignments were identified in the cellulose C4 region (75–92 ppm). For the purposes of this current study one group of peaks was assigned to the crystalline component (89–92 ppm), which to an approximation accounted for all crystallographic splitting from the Cellulose I and II unit cells. A second simulated peak (at approximately 86 ppm) was assigned to the so called partially ordered fraction, thought to be due to surfaces of crystallites, where polymer chains have conformational variability around the pendant C5–C6 bond. A third simulated peak (at 82 ppm) was assigned to the fully disordered fraction, where polymer chains have conformational variability around both C5–C6 and glycosidic bonds.

The crystalline regions of cellulose are anhydrous and therefore should not give rise to any spectral changes as a result of water uptake. However, water should be able to access the partially ordered polymer at the surfaces of crystallites and also the completely disordered polymer fraction. Therefore, changes might be expected in these spectral regions, depending on the equilibrium RH and the overall concentration of water present.

Applying curve fitting to the data at 1 ms contact time, it was found that the ball milled cellulose sample had a small fraction of crystalline material (54% RH: Fig. 7a; Table 5) represented by the small contribution of the composite crystalline peak in the simulation. X-Ray data (not shown), suggests that this is of the order of 5–6%, possibly with both cellulose I and II polymorphs present. Using the longer contact time of 5 ms it was found that the intensity of the simulated peak at 82 ppm due to the completely disordered fraction was substantially lowered, with much less change in the crystalline and partially ordered fractions, according to the simulated peak intensities at 86 and 92 ppm (Fig. 7b). This demonstrates that at these moisture contents the disordered amorphous fraction had substantial mobility in the KHz frequency regime associated with proton $T_{1\rho}$ relaxation. The greater local conformational mobility of this disordered fraction means that the associated relaxation pathway is more effective than in the rigid crystalline fraction so carbon intensity is lost more quickly.

The crystallized material measured at 1 ms contact time (54% RH; after the heating cycle: Fig. 7c) shows the presence of a relatively much larger crystalline peak, however the growth of this is at the expense of the completely disordered fraction. In addition, the 5 ms contact time experiment shows once again little difference in the intensity of the partially ordered peak (86 ppm) but a substantial (threefold) reduction in the completely disordered peak—as for Fig. 7a and b. This shows that the partially ordered fraction has similar mobility to the crystalline material itself, consistent with the conclusions of other work referenced here. This is also probably the reason why despite there being incomplete recrystallization, no evidence for a glass transition is observed on subsequent reheating of a sample in the DMA or DSC. The T_g of this fraction would probably be observed at high temperatures, possibly comparable with the degradation temperatures of the material.

Low resolution proton NMR and sorption behavior

The previously discussed sorption isotherms (Fig. 1) can be useful as an aid to interpret results obtained by low-resolution proton NMR, shown in Fig. 9. From a visual inspection of the isotherm data it appears that discontinuity in behavior exists at a moisture content of approximately 22% db for ball milled cellulose

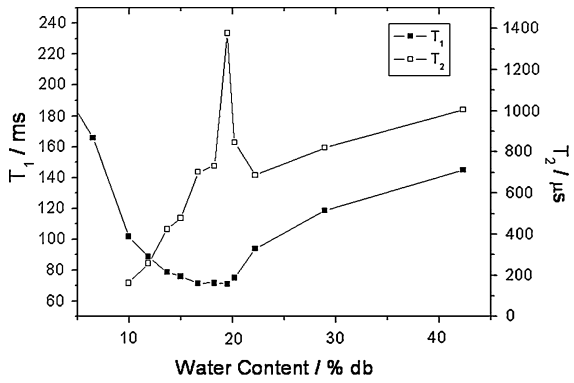

Fig. 9 T_2 and T_1 values for ball milled eucalyptus cellulose as a function of water content (db). Notice that the maximum in T_2 and the minimum in T_1 both occur at approximately 20% moisture content (db)

(around 90% RH from Fig. 1a), where sorption suddenly increases rapidly with RH. This can be modeled via the GAB sorption model as a contribution from the multilayer term, but could also be a result of capillary condensation into smaller voids. This additional water is apparently necessary to provide sufficient conformational freedom to allow effective crystallization of cellulose. Kimura et al. (1974) showed in their work that the rate of recrystallization increased dramatically for amorphous cellulose in this water content range, with the time for recrystallisation decreasing from 6,000 through 4,000 to 300 min at ambient temperature as the humidity changed from 80 through 90 to 100% RH.

The low resolution NMR data presented here show a maximum in the T_2 and a minimum in the T_1 values at this moisture content. Maxima in T_2 values have been associated with the onset of exchange mechanisms. Above a certain water content it is possible for a network of water molecules to form and the bonds to flip between molecules in such a way that the protons previously on biopolymers can be transferred to molecules of water. This is the onset of chemical exchange and is frequently catalyzed by hydrogen ions and hence pH dependent. It also means that instead of the T_2 progressively increasing in value, there is suddenly an averaging with a fraction that was previously invisible to the experiment—often the value of the T_2 of protons on biopolymers is sufficiently low that CPMG echo times are not short enough to detect the decay. This averaging produces a sudden drop in value, which thereafter progressively increases again as the general motion in the system increases with the addition of more water. With regard to T_1, there are additional direct through space averaging processes, such that the overall T_1 profile with temperature or plasticizer content is a broadened minimum—an average of all processes with many different correlation times. The sudden presence of the additional bulk liquid component above 80–90% RH can then contribute to the increase in T_1 as the motional regime now lies on the liquid side of the T_1 minimum.

Conclusions

Using a multitechnique approach, we have demonstrated the crystallization of ball milled cellulose into a mixture of Type I and Type II cellulose, with the subsequent redistribution of the water in the material. The presence of a glass transition has also been shown by mechanical methods using the DMA materials pocket technique. Difficulties in measuring glass transitions in these types of materials, especially with calorimetric techniques, have been highlighted. The existence of fractions with varying degrees of order and mobility has been shown using CPMAS NMR. At water contents in the region of 20% db (RH 80–90%) more than one technique detected large change in properties: Sorption isotherms showed the presence of capillarity water, DSC on recrystallized material showed a freezable fraction of water and low resolution proton NMR showed a maximum in T_2 and a minimum in T_1, which was interpreted as the onset of proton exchange. At water contents higher than 19% db (RH $>$ 80%) recrystallization occurred at room temperature.

Acknowledgments We acknowledge the help of Tim Benson (Advanced Magnetic Resonance Ltd.) in the setting up and maintenance of the NMR equipment. We thank Dr. Andreas Bohn (Fraunhofer Institute, Germany) for preparing the ball milled softwood cellulose and molecular weight determination.

References

Ago M, Endo T, Hirotsu T (2004) Crystalline transformation of native cellulose from cellulose I to cellulose ID polymorph by a ball-milling method with a specific amount of water. Cellulose 11:163–167

Agrawal AM, Manek RV, Kolling WM, Neau SH (2004) Water distribution studies within microcrystalline cellulose and chitosan using differential scanning calorimetry and dynamic vapor sorption analysis. J Pharm Sci 93:1766–1779

Appelqvist IAM, Cooke D, Gidley MJ, Lane SJ (1993) Thermal properties of polysaccharides at low moisture: 1—an endothermic melting process and water–carbohydrate interactions. Carbohydr Polym 20:291–299

Batzer H, Kreibich UT (1981) Influence of water on thermal transitions in natural polymers and synthetic polyamides. Polym Bull 5:585–590

Bhuiyan MTR, Hirai N, Sobue N (2000) Changes of crystallinity in wood cellulose by heat treatment under dried and moist conditions. J Wood Sci 46:431–436

Bizot H, Le Bail P, Leroux B, Davy J, Roger P, Buleon A (1997) Calorimetric evaluation of the glass transition in hydrated, linear and branched polyanhydroglucose compounds. Carbohydr Polym 32:33–50

Chen W, Lickfield GC, Yang CQ (2004) Molecular modeling of cellulose in amorphous state. Part i: model building and plastic deformation study. Polymer 45:1063–1071

Couchman PR, Karasz FE (1978) A classical thermodynamic discussion of the effect of composition on glass-transition temperatures. Macromolecules 11:117–119

Despond S, Espuche E, Cartier N, Domard A (2005) Hydration mechanism of polysaccharides: a comparative study. J Polym Sci B Polym Phys 43:48–58

Drechsler U, Radosta S, Vorwerg W (2000) Characterization of cellulose in solvent mixtures with *N*-methylmorpholine-*N*-oxide by static light scattering. Macromol Chem Phys 201:2023–2031

Dumitriu S (2005) Polysaccharides. Structural diversity and functional versatility. Marcel Dekker, New York

Earl WL, VanderHart DL (2002) Observations by high-resolution carbon-13 nuclear magnetic resonance of cellulose I related to morphology and crystal structure. Macromolecules 14:570–574

Furuta Y, Obata Y, Kanayama K (2001) Thermal-softening properties of water-swollen wood: the relaxation process due to water soluble polysaccharides. J Mater Sci 36:887–890

Gidley MJ, Cooke D, Wardsmith S (1993) 53rd Easter school on glassy state in foods, Nottingham, England, pp 303–316

Goring D (1963) Thermal softening of lignin, hemicellulose and cellulose. Pulp Pap Mag Canada 64:517–527

Hatakeyama H, Hatakeyama T (1981) Structural change of amorphous cellulose by water- and heat-treatment. Makromol Chem 182:1655–1668

Hermans PH, Weidinger A (1946) On the recrystallization of amorphous cellulose. J Am Chem Soc 68:2547–2552

Howsmon JA, Marchessault RH (1959) The ball-milling of cellulose fibers and recrystallization effects. J Appl Polym Sci 1:313–322

Ibbett RN, Domvoglou D, Fasching M (2007) Characterisation of the supramolecular structure of chemically and physically modified regenerated cellulosic fibres by means of high-resolution Carbon-13 solid-state NMR. Polymer 48:1287–1296

Ibbett R, Taylor J, Schuster K, Cox M (2008) Interpretation of relaxation and swelling phenomena in lyocell regenerated cellulosic fibres and textiles associated with the uptake of solutions of sodium hydroxide. Cellulose 15:393–406

Kargin VA, Kozlov PV, Van NC (1960) Classification temperature of cellulose. Dokl Akad Nauk SSSR 130:356–358

Kent M, Meyer W (1984) Complex permittivity spectra of protein powders as a function of temperature and hydration. J Phys D Appl Phys 17:1687–1698

Kimura M, Nakano J (1976) Mechanical relaxation of cellulose at low temperatures. J Polym Sci C Polym Lett 14:741–745

Kimura M, Hatakeyama T, Nakano J (1974) DSC study on recrystallization of amorphous cellulose with water. J Appl Polym Sci 18:3069–3076

Kocherbitov V, Ulvenlund S, Kober M, Jarring K, Arnebrant T (2008) Hydration of microcrystalline cellulose and milled cellulose studied by sorption calorimetry. J Phys Chem B 112:3728–3734

Kubat J, Pattyran C (1967) Transition in cellulose in the vicinity of −30 °C. Nature 215:390–391

Larsson T, Wickholma K, Iversena T (1997) A CP/MAS ^{13}C NMR investigation of molecular ordering in celluloses. Carbohydr Res 302:10–25

Lazaridou A, Biliaderis CG, Kontogiorgos V (2003) Molecular weight effects on solution rheology of pullulan and mechanical properties of its films. Carbohydr Polym 52:151–166

Lomauro GJ, Bakshi AS, Labuza TP (1985) Evaluation of food moisture sorption isotherms equations. Part I: fruit, vegetables and meat products. Lebensm Wiss Technol 18:111–117

Maier G, Zipper P, Stubicar M, Schurz J (2005) Amorphization of different cellulose samples by ball milling. Cellul Chem Technol 39:167–177

Matsuda Y, Kowsaka K, Okajima K, Kamide K (1992) Structural change of cellulose contained in immature cotton boll during its growth. Polym Int 27:347–351

Mazeau K, Heux L (2003) Molecular dynamics simulations of bulk native crystalline and amorphous structures of cellulose. J Phys Chem B 107:2394–2403

Montes H, Mazeau K, Cavaille JY (1997) Secondary mechanical relaxations in amorphous cellulose. Macromolecules 30:6977–6984

Newman RH, Hemmingson JA (1995) Carbon-13 NMR distinction between categories of molecular order and disorder in cellulose. Cellulose 2:95–110

Noel TR, Parker R, Brownsey GJ, Farhat IA, MacNaughtan W, Ring SG (2005) Physical aging of starch, maltodextrin, and maltose. J Agric Food Chem 53:8580–8585

Ogiwara Y, Kubota H, Hayashi S, Mitomo N (1970) Temperature dependency of bound water of cellulose studied by a high resolution NMR spectrometer. J Appl Polym Sci 14:303

Orford PD, Parker R, Ring SG, Smith AC (1989) Effect of water as a diluent on the glass-transition behavior of malto-oligosaccharides, amylose and amylopectin. Int J Biol Macromol 11:91–96

Ouajai S, Shanks RA (2006) Solvent and enzyme induced recrystallization of mechanically degraded hemp cellulose. Cellulose 13:31–44

Öztürk H, Potthast A, Rosenau T, Abu-Rous M, MacNaughtan B, Schuster K, Mitchell J, Bechtold T (2009) Changes in the intra- and inter-fibrillar structure of lyocell (TENCEL®) fibers caused by NaOH treatment. Cellulose 16:37–52

Perez-Alonso C, Beristain CI, Lobato-Calleros C, Rodriguez-Huezo ME, Vernon-Carter EJ (2006) Thermodynamic analysis of the sorption isotherms of pure and blended carbohydrate polymers. J Food Eng 77:753–760

Purves CB (1954) Chain structure in cellulose and cellulose derivatives. Wiley-Interscience, New York

Rahman S (1995) Food properties handbook. CRC Press, Boca Raton

Raschip IE, Yakimets I, Martin CP, Paes SS, Vasile C, Mitchell JR (2008) Effect of water content on thermal and dynamic mechanical properties of xanthan powder: a comparison between standard and novel techniques. Powder Technol 182:436–443

Rizvi SSH (1994) Thermodynamics properties of foods in dehydration. In: Rao MA, Rizvi SSH (eds) Engineering

properties of foods, 2nd edn. Marcel Dekker, Inc., New York, pp 223–310

Roos YH (1995) Phase transition in foods. Academic Press, San Diego

Royall PG, Huang CY, Tang SWJ, Duncan J, Van-de-Velde G, Brown MB (2005) The development of DMA for the detection of amorphous content in pharmaceutical powdered materials. Int J Pharm 301:181–191

Salmen NL, Back EL (1977) Influence of water on glass-transition temperatures of cellulose. Tappi 60:137–140

Shogren RL (1992) Effect of moisture-content on the melting and subsequent physical aging of cornstarch. Carbohydr Polym 19:83–90

Stratton RA (1973) Dependence of the viscoelastic properties of cellulose on water content. J Polym Sci A Polym Chem 11:535–544

Stubberud L, Arwidsson HG, Larsson A, Graffner C (1996) Water solid interactions II. Effect of moisture sorption and glass transition temperature on compactibility of microcrystalline cellulose alone or in binary mixtures with polyvinyl pyrrolidone. Int J Pharm 134:79–88

Stute R (1992) Hydrothermal modification of starches: the difference between annealing and heat/moisture -treatment. Starch Stärke 44:205–214

Szczesniak L, Rachocki A, Tritt-Goc J (2008) Glass transition temperature and thermal decomposition of cellulose powder. Cellulose 15:445–451

Van den Berg C (1984) Description of water activity of foods for engineering purposes by means of the GAB model of sorption. In: McKenna BM (ed) Engineering and food. Elsevier Applied Science, New York, pp 311–321

Van den Berg C, Bruin S (1981) Water activity: influence on food quality. Academic Press, New York

Wadehra IL, Manley RSJ (1965) Recrystallization of amorphous cellulose. J Appl Polym Sci 9:2627–2630

Yakimets I, Paes SS, Wellner N, Smith AC, Wilson RH, Mitchell JR (2007) Effect of water content on the structural reorganization and elastic properties of biopolymer films: a comparative study. Biomacromolecules 8:1710–1722